

## FATIGUE-CRACK PROPAGATION OF LASER SURFACE REMELTED NODULAR CAST IRON<sup>1</sup>

Roman Šturm<sup>2</sup>  
Janez Grum<sup>3</sup>

### Abstract

Laser surface remelting (LSR) of nodular cast iron is applied to surface modification and is suitable for manufacture of various machine and tool parts. Usually studies of remelted layers include microstructural and microchemical analyses and occasionally, if the research is exact, also measurements of residual stresses, various wear and corrosion tests. This paper will represent microstructural analyses of the thin surface layer after laser remelting of nodular cast iron 500-7, and further on also the micro-hardness profile. A particular attention is paid to fatigue-crack initiation and propagation tests. The comparison is made between as received nodular cast iron 500-7 and the same material altered with laser surface remelting process. As the crack propagation is normal to the laser remelted layer, the specimens with laser remelted surface of nodular cast iron exhibited higher resistance to fatigue-crack growth in the low stress intensity factor range  $\Delta K_{th}$  than as-received nodular cast iron specimens. Also  $\Delta K_{IC}$  is higher in the case of laser remelted surface.

**Keywords:** Laser surface remelting; Nodular cast iron; Fatigue; Crack propagation.

<sup>1</sup> Technical contribution to the 18<sup>th</sup> IFHTSE Congress - International Federation for Heat Treatment and Surface Engineering, 2010 July 26-30<sup>th</sup>, Rio de Janeiro, RJ, Brazil.

<sup>2</sup> Faculty of Mechanical Engineering, Aškerčeva 6, 1000 Ljubljana, Slovenia. roman.sturm@fs.uni-lj.si, University of Ljubljana.

<sup>3</sup> Faculty of Mechanical Engineering, Aškerčeva 6, 1000 Ljubljana, Slovenia. janez.grum@fs.uni-lj.si, University of Ljubljana.

## INTRODUCTION

In the recent years, there has been a considerable increase of engine performances and efficiency through surface engineering. Laser surface remelting of cast irons is an attractive process developing corrosion and/or wear resistant layers, due to the inherent rapid solidification and high concentration of carbon, combined with a good metallurgical bonding to the base metal. Industrial applications include mainly CO<sub>2</sub> and Nd-YAG laser sources that provide appropriate power, and consequently, energy density required for carrying out materials processing.

Laser surface remelting is of commercial interest because of its ability to alter with accuracy the properties of localized surface regions without reprocessing the material as a whole.<sup>[1]</sup> By choosing a suitable energy input,<sup>[2]</sup> we can achieve rapid local heating up to the austenitic region or even the temperature of the surface layer melting which, after the cooling process is completed, enables us to obtain a modified layer of desired depth.<sup>[3]</sup> Rapid heat transfer into the remaining part of the cold mass can quite easily achieve the required surface layer cooling rates.<sup>[4]</sup> Thus, the aim of surface remelting process is to ensure a fine-grained microstructure with uniform microhardness, which cannot be achieved by other procedures for surface hardening of pearlite-ferrite cast irons.<sup>[5]</sup> The properties of the modified layer depend on the microstructure prior to heat treatment and on the amount of energy input transferred to the surface layer of the specimen.<sup>[6,7]</sup> This study discusses the different effects of the laser remelting process on the microstructural changes in the surface layer as well as residual stresses developed in the nodular cast iron 500-7.

The next step is to investigate the fatigue crack propagation of the material. Korda et al.<sup>[8]</sup> investigated the effect of pearlite morphology on fatigue crack growth behavior in ferritic-pearlitic structural steels with no additional surface heat treatment process. They found out, that islands of pearlite colonies in the microstructure reduce fatigue crack growth resistance. Then, Tsay et al.<sup>[9,10]</sup> found out, that laser surface remelted specimens with no additional welding material exhibited a higher resistance to crack growth in the low stress intensity factor range  $\Delta K$  than the as-received steel plates, regardless of testing environments. Fractographic examinations indicated the existence of transgranular and intergranular fracture modes in the surface remelted metal. Similarly, Hwang et al.<sup>[11]</sup> studied the effect of electron beam surface hardening on the fatigue crack growth rate in steel. Electron beam surface hardening increases compressive residual stress in the hardened layer and thus improves the fatigue crack growth resistance. In addition to this, Rubio-Gonzalez et al.<sup>[12]</sup> and Xu et al.,<sup>[13]</sup> described effects of different lasers surface modification processes on fatigue crack resistance of relatively soft aluminum alloys. Laser shock processing and laser surface melting induces a compressive residual stress field which increases fatigue crack initiation life and reduces fatigue crack growth rate, and increases fracture toughness in aluminum alloys. Very little effort has been devoted to research on mechanical properties such as fatigue behavior of cast iron with remelted surface.

Therefore, the main aim of this paper is to evaluate specimens of nodular iron 500-7 with laser remelted surface on fatigue properties as they are crack initiation and propagation. The prime objectives in development of advanced surface layers are to improve the surface quality and to extend the life of the component. To achieve these objectives, it is essential to understand fracture properties which directly affect the life of altered surface component.

## EXPERIMENTAL PROCEDURE

For experimental testing of the laser surface remelting procedure, nodular cast iron 500-7 (according to ISO standard) was used, having a pearlite-ferrite matrix (31% of pearlite and 69% of ferrite) that contains graphite nodules. Nodular iron 500-7 contains 10.76 vol. % of graphite nodules. The average diameter of graphite nodules was 30  $\mu\text{m}$ . The chemical composition of the investigated nodular cast iron was: C=3.77 %, Si=2.26 %, Ni=0.03 %, Cr=0.04 %, Cu=0.33 %, Mn=0.13 % in wt. %, and carbon equivalent was CE=4.53. Laser light absorptivity of the specimen surface<sup>[14]</sup> was increased by treating the specimen surface in a Zn-phosphate bath for 10' at 50°C. The laser surface remelting tests were performed with a CO<sub>2</sub> laser, with a maximum working power of 1.5 kW and a Gaussian distribution of energy in the beam. The tests were made with a laser power of 1.0 kW, the focal length of the focusing lens was 127 mm, and the defocusing distance of the beam was 22 mm. The laser beam travelling speed was 21 mm/s. The energy input into the specimen material achieved with these laser parameters was 14.4 J/mm<sup>2</sup>, which was preliminary found out as the optimal energy input for our material.

The energy input provided the remelting of a thin surface layer. In this case the microstructure of the modified surface layer consists of the remelted and hardened layer. The average depth of the remelted layer was between 0.3 and 0.4 mm and the average depth of the whole modified layer was between 0.6 and 0.8 mm.

To achieve a fully remelted surface area of the specimen, the kinematics of the laser beam were adapted so that a 30 % overlapping of the width of the remelted traces was ensured. The overlapping in the remelted surface is expressed in percent with respect to the width of a single remelted trace. In laser remelting process argon was used as an assistant gas in amount of 3 – 6 l/min. The test specimens were laser remelted on one side of the surface. Then the test specimens were cut in laser movement direction to 10 mm wide samples, which were prepared as Charpy-V specimens (60 x 10 x 8 mm). 2 mm deep V-notch was placed perpendicular to laser remelted surface. Figure 1 shows a schematic illustration of laser surface remelting experiment and specimen preparation for fatigue testing.

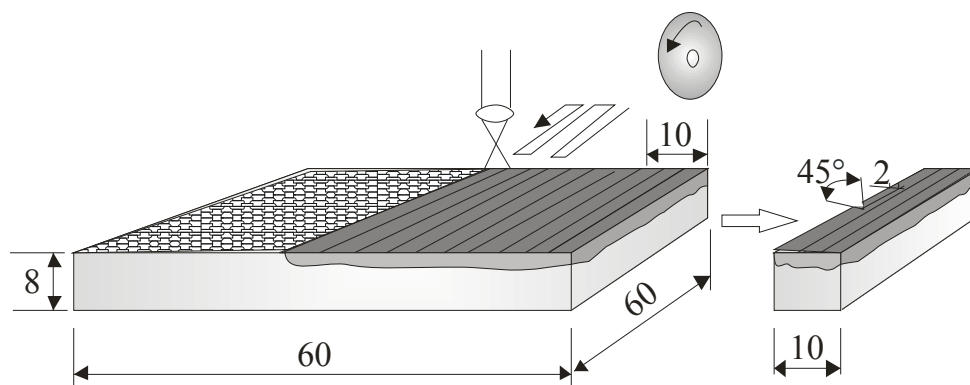


Figure 1. Schematic illustration of laser surface remelting experiment.

Such Charpy-V specimens were then subjected to fatigue tests in as plain nodular iron 500-7 condition, and also in as laser surface remelted condition. All fatigue tests were carried out on an electro-magnetic resonance fatigue testing machine of type Cracktronic from Rumul Russenberger Prüfmaschinen AG, Switzerland. The program package allowed computer controlled fatigue tests, and the

crack length was measured with a device Fractomat. Measurements of crack propagation were made according to standard ASTM E-647. The tests were performed in the regime of decreasing stress intensity factor  $\Delta K$  at constant stress ratio of  $R = 0.1$ . The stress induced in the specimen, and the high cyclic movement of the specimen was controlled with a device Cracktronic. The testing frequency was about 180 Hz, the resonance frequency of our Charpy-V specimens. Figure 2 shows a schematic illustration of resonance fatigue testing experiment. Measurements of crack length and crack growth were done with a help of resistance strain gages RMF-A5, which were glued on the laser alloyed surface over the V-notch. When a crack initiates and propagates, the special resistant strain gage RMF-A5 tears apart corresponding to the crack length and the change in electrical resistance measured with Fractomat tells us the actual crack length with 0.01 mm accuracy.

A computer program collected the electrical potential drop change in resistant strain gage, and the elapsed number of cycles. Additionally, the overall crack lengths after the tests were measured within the optical microscope and were compared with the obtained values by resistant strain gages, which were in good agreement. The fatigue crack propagation tests were stopped when  $da/dN$  of about  $5 \cdot 10^{-11}$  m/cycle was reached.

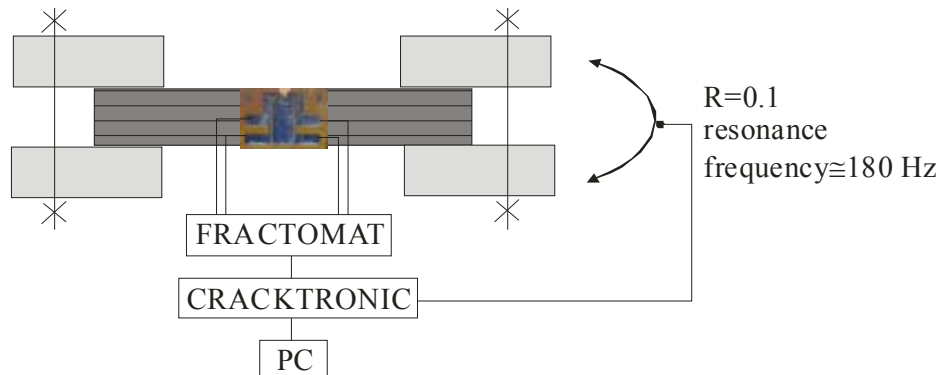


Figure 2. Schematic illustration of resonance fatigue testing experiment.

## RESULTS

### Microstructure of the Laser Surface Remelted Layer

Figure 3 shows the microstructure changes in the modified layer of the nodular iron 500-7. The modified layer consists of two characteristic microstructure layers: remelted layer and hardened layer.

#### Remelted Layer

During laser surface remelting of nodular iron 500-7, at the interface between the molten and the solid condition, a very high solidification rate is achieved during self-cooling. The conditions during solidification are mainly controlled by the crystal growth rate over the interface temperature in the molten pool, where the temperature gradient plays a very important role.

It was confirmed that remelted surface of nodular cast iron 500-7 consisted of retained austenite ( $Fe_\gamma$ ), martensite ( $Fe_\alpha'$ ), cementite ( $Fe_3C$ ) and graphite (C). Very

rapid cooling rates of the thin surface remelted layer of the nodular cast iron can, depending on the remelting conditions, produce the following effects:

- Incomplete dissolution of graphite nodules;
- Redistribution of larger undissolved graphite nodules as a result of hydrodynamic and buoyancy forces in the molten pool;
- The hydrodynamic forces acting on the molten pool cause the pool to agitate and thus homogenize. After the laser beam has passed the specimen surface, the melt undergoes a solidification process caused by heat transfer from the molten pool beyond the melt solid interface.

### Hardened Layer

In the hardened layer, transformations occur during laser heating in the solid state. During the laser heating, the pearlite matrix transforms into a carbon rich austenite microstructure, into which additional carbon diffuses from graphite nodules. During rapid self-cooling or self-quenching, the carbon rich austenite microstructure transforms into martensite with some residual austenite.

The ferrite matrix transforms during laser heating into an austenite microstructure without carbon, or with very low portions. At high temperatures carbon diffuses in the austenite very fast. Thus, during rapid cooling, hard ledeburite and/or martensite shells form surrounding graphite nodules,<sup>[15]</sup> as it could be seen in the hardened layer in Figure 3.

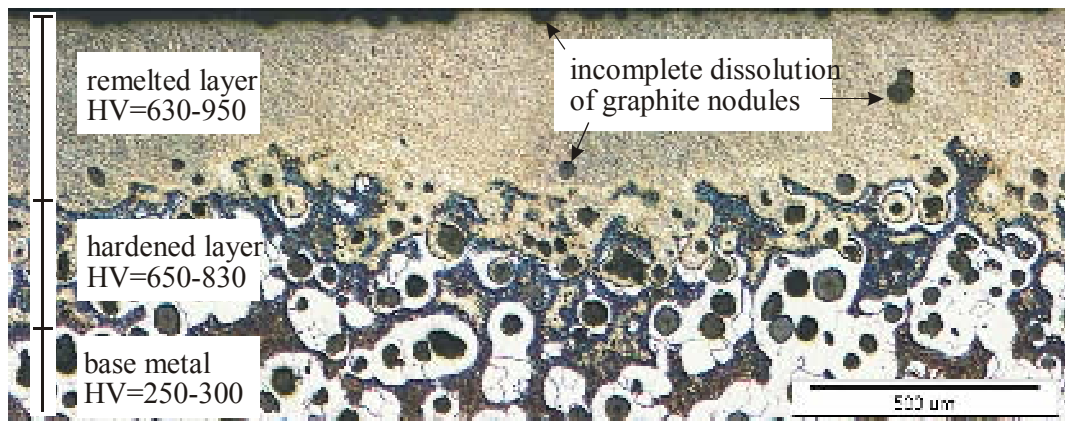


Figure 3. Microstructure of the surface modified layer.

### Microhardness Analysis

The results of microhardness measurements have confirmed the microstructure changes in the material and have shown that laser surface remelting can be a successful method. The microhardness of the bulk pearlite material is between 250 and 300 HV<sub>0.1</sub> and after laser treatment increases to range between 630 and 950 HV<sub>0.1</sub> in the remelted layer and to range between 650 and 830 HV<sub>0.1</sub> in the martensite microstructure of the hardened layer (Figure 4).

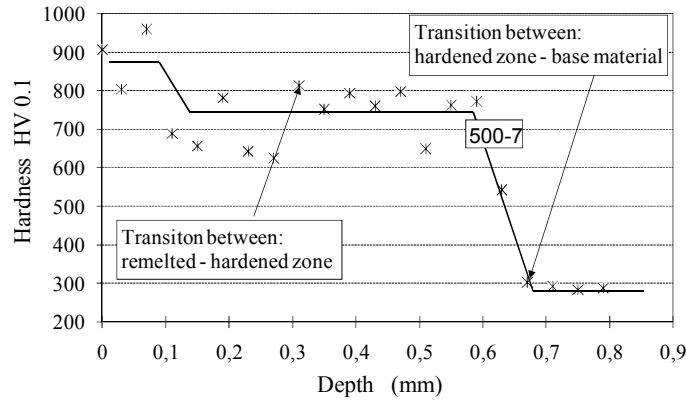


Figure 4. Microhardness measurements cross the modified layer of laser remelted surface.

### Residual Stresses

The knowledge about the stress state in the surface remelted and heat affected layer is very often essential for parts which are subjected to dynamical loads. In Figure 5 we can see the variation of residual stresses in the modified layer of nodular iron 500-7. From the results in Figure 5 we can conclude the following:

- Residual stresses have in the surface remelted layer tensile character in a range between 50 and 150 MPa.
- The change from tensile into compressive residual stresses takes place in the lower part of the remelted layer. Maximum compressive residual stress values were found in the middle of the hardened layer in a range between -25 and -70 MPa.

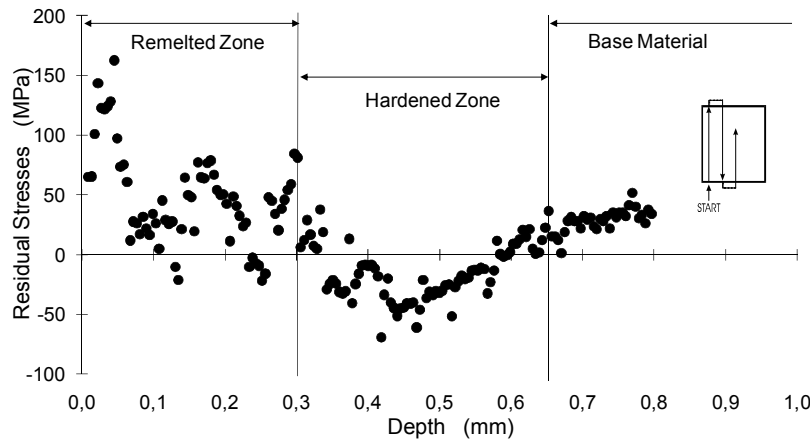


Figure 5. Residual stresses in modified layer of nodular iron 500-7 after surface remelting process.

### Fatigue Crack Growth Behavior

Figure 6 shows fatigue crack growth curves for the nodular iron 500-7 in as-received state and altered with laser surface remelting procedure (LSR). The fatigue crack growth rate ( $da/dN$ ) vs. the variation in stress intensity factor range ( $\Delta K$ ) was plotted in log-log diagrams, where  $da/dN$  is evaluated from the slope of  $a-N$  curve.

Comparing the curves in Figure 6, one sees that the fatigue crack growth curve of LSR specimen is shifted well to the right of that of unmodified specimen. The hard surface layer obviously plays an important role to retard the crack threshold stress

intensity factor range. In our Charpy specimens, threshold stress intensity factor range,  $\Delta K_{th}$ , of plain nodular iron 500-7 was obtained as 13.3 MPa m<sup>1/2</sup>. This value was higher in the case of LSR, and was around 17.3 MPa m<sup>1/2</sup>. In Paris regime, fatigue growth resistance was higher in the case of plain nodular iron, due to better toughness. The brittleness of the laser surface remelted layer of nodular iron influenced faster crack propagation in comparison to plain nodular iron. At high stress intensity factor range we can denote the equivalent interface fracture toughness,  $\Delta K_{IC}$ , which is 20.8 MPa m<sup>1/2</sup> for plain nodular iron, and 26.2 MPa m<sup>1/2</sup> for laser surface remelted (LSR) nodular iron.

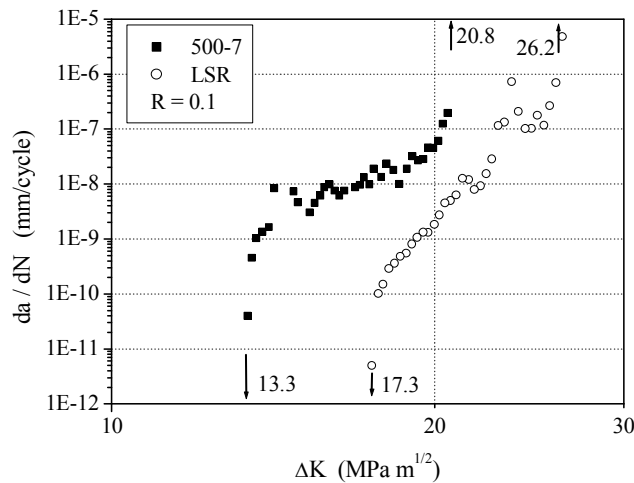


**Figure 6.** Relationship between  $da/dN$  and  $\Delta K$  for plain nodular iron (500-7) and for laser surface remelted nodular iron (LSR).

High strength and high hardness of the laser remelted surface can at the early stage of the crack growth process effectively retard the fatigue crack growth. As the crack initiates and start to grow, the tensile residual stresses in the surface remelted layer and the brittleness of the hardened layer affect the increase of crack growth rate.

In Figure 7 we can see additional data about the fracture mechanisms at high stress intensity factor range. Figure 7a shows that our tests were performed in the regime of decreasing stress intensity factor  $\Delta K$  at constant stress ratio of  $R = 0.1$ . Our tests started with  $\Delta K_{IC}$  values above 30 MPa m<sup>1/2</sup>. We have found out that for plain nodular iron 500-7  $\Delta K_{IC} = 20.8$  MPa m<sup>1/2</sup> and for LSR nodular iron  $\Delta K_{IC} = 26.2$  MPa m<sup>1/2</sup>. At that stress intensity factor range the crack at the surface initiates and starts to grow. Figure 7a shows that initial crack length in the case of plain nodular iron was 0.2 mm, and 0.8 mm in the case of LSR nodular iron. The difference between plain nodular iron and LSR nodular iron is also in number of cycles, which are needed for crack initiation. Figure 7b shows that in the case of LSR nodular iron, the number of cycles needed for crack initiation is  $N=3.7 \cdot 10^2$  and is lower than in the case of plain nodular iron 500-7, where the number of cycles needed for crack initiation is  $N=7.7 \cdot 10^2$ .

The high hardness of microstructure of the surface remelted layer (LSR nodular iron) can restrict the deformation of the base material. Because of that such a specimen needs higher fracture toughness stress level for crack initiation. If we compare curves in Figure 7b, we can find out, that at the fracture toughness  $\Delta K_{IC} = 20.8$  MPa m<sup>1/2</sup> of plain nodular iron, the expected number of cycles for crack

initiation in LSR nodular iron is much higher and is around  $N=8 \cdot 10^4$ . But when crack initiates, it propagates faster through a brittle material.

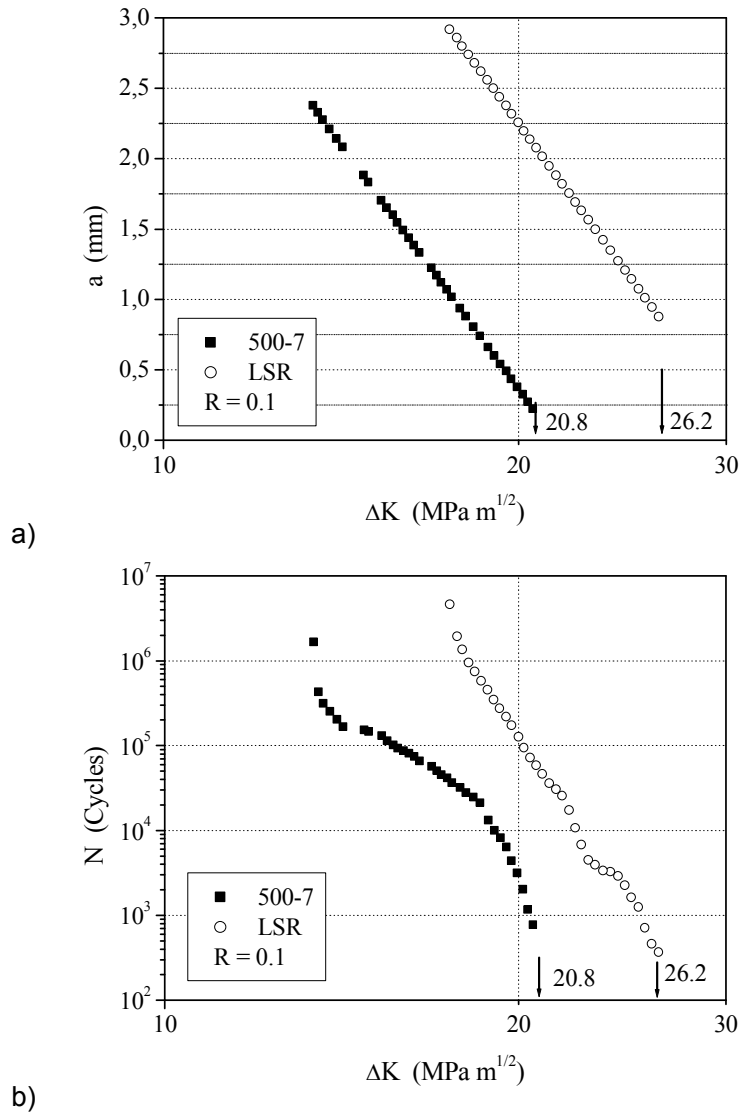


**Figure 7.** Relationship between decreasing stress intensity factor  $\Delta K$  versus crack length  $a$  (a) and number of cycles  $N$  (b).

In general, the ratio of threshold to fracture toughness,  $\Delta K_{th}/\Delta K_{IC}$ , in brittle metals is of high magnitude, while the ratio in ductile materials is of relatively low magnitude. In other words,  $\Delta K_{th}/\Delta K_{IC}$  represents the brittleness in fatigue growth. In our case,  $\Delta K_{th}/\Delta K_{IC}$  of the LSR nodular iron is 0.65, and which is almost the same as that of plain nodular iron 0.63.

The influence of microstructure in cross-section of the specimen on fatigue-crack growth resistance in Paris regime is described with Equation 1:

$$da/dN = C (\Delta K)^m \quad (1)$$

where  $da/dN$  – fatigue crack growth rate,  $\Delta K$  – the stress intensity factor range,  $C$  and  $m$  – material constants. The results of such an equation can be used to predict the



fatigue life of a component. In Table 1 parameters of the fatigue crack growth rate model are presented for plain nodular iron 500-7 and for LSR nodular iron.

**Table 1.** Parameters of the fatigue crack growth model

Material	$\Delta K_{th}$ (MPa m <sup>1/2</sup> )	C	m	$\Delta K_{IC}$ (MPa m <sup>1/2</sup> )
Plain nodular iron 500-7	13.3	$2 \cdot 10^{-16}$	6.38	20.8
LSR nodular iron	17.3	$8 \cdot 10^{-21}$	8.96	26.2

## CONCLUSIONS

Results of microhardness and microstructural research showed that, in the laser surface remelted layer of nodular iron 500-7, desired microstructure with hardness between 630 HV<sub>0.1</sub> and 950 HV<sub>0.1</sub> was obtained. However, residual stresses have rose in the material after uneven heating and cooling of laser processing. The laser surface remelting process induces residual stress variation in the modified surface layer, which depend greatly on remelting conditions. Phase transformations causing a reduction in the volume of the remelted layer give rise to tensile residual stresses of even 150 MPa in it. On the other hand, in the hardened layer martensite transformation causes an increase in volume and contributes to compressive residual stresses of maximum –70 MPa.

Fatigue crack growth tests were performed to evaluate fatigue behavior of plain nodular iron specimens with or without laser surface remelting process. As the crack propagation is normal to the laser remelting or scan direction, the laser surface remelted specimens exhibited a higher resistance to crack growth in the low stress intensity factor range ( $\Delta K_{th}$ ) than the as-received nodular iron. The high hardness of microstructure of the surface remelted layer restrict the deformation of the specimen, which hold back crack initiation and crack growth at the low stress intensity factor range  $\Delta K_{th}$  from value of 13.3 MPa m<sup>1/2</sup> in plain nodular iron to value  $\Delta K_{th} = 17.3$  MPa m<sup>1/2</sup> in LSR nodular iron.

On the basis of our results it could be concluded, that laser surface remelting process of nodular iron 500-7 is a suitable process for applying in dynamical loaded parts, because obtained surface layer is of high average hardness over 750 HV<sub>0.1</sub>. Although surface remelted layer has unfavorable tensile residual stresses of average amount of 50 MPa, all together in our case influences the increase of threshold stress intensity factor range  $\Delta K_{th}$  for 30%.

## REFERENCES

- 1 H.W. Bergmann: Current Status of Laser Surface Melting of Cast Iron, Surface Engineering, 1985, Vol. 1, (2) 137-155.
- 2 R. Vilar, J. S. Figueira, R. Sabino: Laser Surface Melting of Cast Iron, Eclat'90, 1990, Surface Treatments – Liquid State, 593-604.
- 3 Y. Guan, J.P. Montagnon, D. Pantelis, Ph. Popupeau, D. Francois: Laser Surface Treatment of Ferrite-pearlitic Spheroidal Graphite Cast Iron, -Memoires et Etudes Scientifiques Revue de Metallurgie, 1990, Vol. 87, (1), 21-32.
- 4 Y.P. Lei, H. Murakawa, Y.W. Shi, X.Y. Li: Numerical Analysis of the Competitive Influence of Marangoni Flow and Evaporation on Heat Surface Temperature and Molten Pool Shape in Laser Surface Remelting, Computational Materials Science, 21, 2001, 276-290.

- 5 K.Y. Benyounis, O.M.A. Fakron, J.H. Abboud, A.G. Olabi, M.J.S. Hashmi: Surface Melting of Nodular Cast Iron by Nd-YAG Laser and TIG, *Journal of Materials Technology*, 170, 2005, 127-132.
- 6 H.R. Shercliff and M.F. Ashby: The Prediction of Case Depth in Laser Transformation Hardening, *Metallurgical Transactions A*, 22A, 1991, 2459-2466.
- 7 H. Pantsar: Relationship between Processing Parameters, Alloy Atom Diffusion Distance and Surface Hardness in Laser Hardening of Tool Steel, *Journal of Materials Processing Technology*, 189, 2007, 435-440.
- 8 Korda A.A., Mutoh Y., Miyashita Y., Sadasue T.: Effects of Pearlite Morphology and Specimen Thickness on Fatigue Crack Growth Resistance in Ferritic-Pearlitic Steels, *Materials Science and Engineering A*, Vol. 428, 2006, 262-269.
- 9 Tsay L.W., Chung C.S., Chen C.: Fatigue Crack Propagation of D6AC Laser Welds, *International Journal of Fatigue*, Vol. 19, No. 1, 1997, 25-31.
- 10 Tsay L.W., Young M.C., Chen C.: Fatigue Crack Growth Behavior of Laser-processed 304 Stainless Steel in Air and Gaseous Hydrogen, *Corrosion Science*, Vol. 45, 2003, 1985-1997.
- 11 Hwang J.R., Fung C.P.: Effect of Electron Beam Surface Hardening on Fatigue Crack Growth Rate in AISI 4340 Steel, *Surface and Coatings Technology*, Vol. 80, 1996, 271-278.
- 12 Rubio-Gonzales C., Ocaza J.L., Gomes-Rosas G., Molpeceres C., Paredes M., Banderas A., Porro J., Morales M.: Effect of Laser Shock Processing on Fatigue Crack Growth and Fracture Toughness of 6061-T6 Aluminium Alloy, *Materials Science and Engineering A*, Vol. 386, 2004, 291-295.
- 13 Xu W.L., Yue T.M., Man H.C., Chan C.P.: Laser Surface Melting of Aluminium Alloy 6013 for Improving Pitting Corrosion Fatigue Resistance, *Surface & Coatings Technology*, Vol. 200, 2006, 5077-5086.
- 14 H. Jiang, P. Woodard: Methodology of Generic Modeling as Applied to Energy Coupling of CO<sub>2</sub> Laser Material Interaction, *Optics and Lasers in Engineering*, 43, 2005, 19-31.
- 15 M. Tsujikawa, M. Hino, M. Kawamoto, K. Okabayashi: "Hard – Eye" Ductile Cast Iron and its Treatment by Laser Quenching, *Congress Book: The 8<sup>th</sup> Congress on Heat Treatment of Materials, Heat & Surface'92*, 1992, Ed.: Tamura, Tokyo, Japan, 441-444.